

## Identification of shell-model states in $^{135}\text{Sb}$ populated via $\beta^-$ decay of $^{135}\text{Sn}$

J. Shergur,<sup>1,2</sup> A. Wöhr,<sup>1,3</sup> W. B. Walters,<sup>1</sup> K.-L. Kratz,<sup>4</sup> O. Arndt,<sup>4</sup> B. A. Brown,<sup>5</sup> J. Cederkall,<sup>6</sup> I. Dillmann,<sup>4</sup> L. M. Fraile,<sup>6,7</sup> P. Hoff,<sup>8</sup> A. Joinet,<sup>6</sup> U. Köster,<sup>6</sup> and B. Pfeiffer<sup>4</sup>

<sup>1</sup>*Department of Chemistry, University of Maryland, College Park, Maryland 20742-2021, USA*

<sup>2</sup>*Physics Division, Argonne National Laboratory, Argonne, Illinois 60439, USA*

<sup>3</sup>*Department of Physics, University of Notre Dame, Notre Dame, Indiana 46556, USA*

<sup>4</sup>*Institut für Kernchemie, Universität Mainz, D-55128 Mainz, Germany*

<sup>5</sup>*Department of Physics and Astronomy and National Superconducting Cyclotron Laboratory, Michigan State University, East Lansing, Michigan 48824-1321, USA*

<sup>6</sup>*ISOLDE, PH Department, CERN, CH-1211 Genève 23, Switzerland*

<sup>7</sup>*Departamento de Física Atómica Molecular y Nuclear, Universidad Complutense, E-28030 Madrid, Spain*

<sup>8</sup>*Department of Chemistry, University of Oslo, NO-1163 Oslo, Norway*

(Received 14 March 2005; published 12 August 2005)

The  $\beta$  decay of  $^{135}\text{Sn}$  was studied at CERN/ISOLDE using a resonance ionization laser ion source and mass separator to achieve elemental and mass selectivity, respectively.  $\gamma$ -ray singles and  $\gamma$ - $\gamma$  coincidence spectra were collected as a function of time with the laser on and with the laser off. These data were used to establish the positions of new levels in  $^{135}\text{Sb}$ , including new low-spin states at 440 and 798 keV, which are given tentative spin and parity assignments of  $3/2^+$  and  $9/2^+$ , respectively. The observed levels of  $^{135}\text{Sb}$  are compared with shell-model calculations using different single-particle energies and different interactions.

DOI: [10.1103/PhysRevC.72.024305](https://doi.org/10.1103/PhysRevC.72.024305)

PACS number(s): 23.40.-s, 23.20.-g, 27.60.+j, 21.60.Cs

### I. INTRODUCTION

Study of the structures and decay of Ag, Cd, In, Sn, Sb, and Te nuclides with  $125 < A < 140$  have taken on new importance in recent years owing to the vital role that these properties play in  $r$ -process nucleosynthesis calculations [1]. Data for nuclides in this mass region that lie directly in the  $r$ -process path are essential for such calculations, and also serve to test models that must be used to describe nuclides not yet accessible to experimental measurements. For example, Dillmann *et al.* recently reported new measurements for the  $Q$  value and decay of  $^{130}\text{Cd}$  that revealed significant divergence from many mass models whose values are widely used as input parameters for abundance calculations [2].

In addition to astrophysical implications of the decay properties of these Sn nuclides, the low-energy level structures of the nuclides that have two or three particles or holes adjacent to the doubly-closed shell nuclide  $^{132}\text{Sn}$  are of particular interest for the determination and testing of two-body matrix elements (TBME) that underlie calculations of nuclides much further from stability [3,4]. In particular, the nuclides  $^{135}\text{I}$ ,  $^{135}\text{Te}$ ,  $^{135}\text{Sb}$ , and  $^{135}\text{Sn}$  remain an excellent testing ground for descriptions of nuclei with only three nucleons present beyond the  $^{132}\text{Sn}$  double shell closure. Relatively detailed data have been available for some time for  $^{135}\text{I}$  and  $^{135}\text{Te}$  [5,6].

The first level structure for  $^{135}\text{Sb}$  was reported by Bhattacharyya *et al.* who identified the yrast cascade up to the  $23/2^+$  level [7]. Low-spin structure for  $^{135}\text{Sb}$  was first reported by Shergur *et al.* [8,9], who identified nine new excited levels below 2.5 MeV. In that experiment, only two low-energy  $\gamma$  rays at 282 and 317 keV were observed owing to the presence of two intense  $\gamma$  rays at 787 and 846 keV arising from the decay of the surface-ionized spallation-product nuclide 53-min  $^{135}\text{Cs}^{\text{m}}$ . Similar, but less detailed data was also published by

Korgul *et al.* for  $^{135}\text{Sn}$  decay [10]. In this paper, new data for the decay of  $^{135-137}\text{Sn}$  are reported that have benefited from technical improvements at ISOLDE that dramatically reduce the presence of spallation-produced Cs and Ba isotopes.

### II. EXPERIMENTAL PROCEDURE

Neutron-rich Sn nuclei were produced at ISOLDE/CERN by high-energy neutron-induced fission of a  $\text{UC}_2$  target (20 cm long, thickness 52 g/cm<sup>2</sup> and  $\sim 10$  g/cm<sup>2</sup> of graphite). The high-energy neutrons were obtained by bombarding a tungsten rod adjacent to the  $\text{UC}_2$  target with 1.4 GeV proton pulses from the Proton Synchrotron Booster (PSB). The proton pulses are delivered with an intensity of  $3 \times 10^{13}$  protons/pulse and extracted as often as every 1.2 s. With this approach, proton-induced spallation in the target is greatly reduced with only minimal reduction in the yields of neutron-rich fission-product nuclei. In addition, ionization of other elements (Te and I) caused by the rapid deposition of energy in the target that accompanies the proton pulse is also minimized.

Following ionization by the resonance ionization laser ion source (RILIS), Sn ions were extracted from the target-ion source and mass separated using the general purpose separator prior to implantation into an Al coated tape in a moving tape station. The point of implantation was located in the center of an array of five HPGe detectors and three plastic scintillators. The plastic scintillators were used to veto  $0^\circ\beta$ - $\gamma$  singles and coincidence events, and, at the same time provide for high efficiency  $\beta$ -gated  $\gamma$  spectra where the  $\beta$  particle has been detected in a different direction from the  $\gamma$  ray. For each event, the outputs of the detectors were recorded along with time-to-amplitude converter information and the time of the event following the proton pulse.  $\gamma$ -singles,  $\gamma$ - $\gamma$  coincidence,

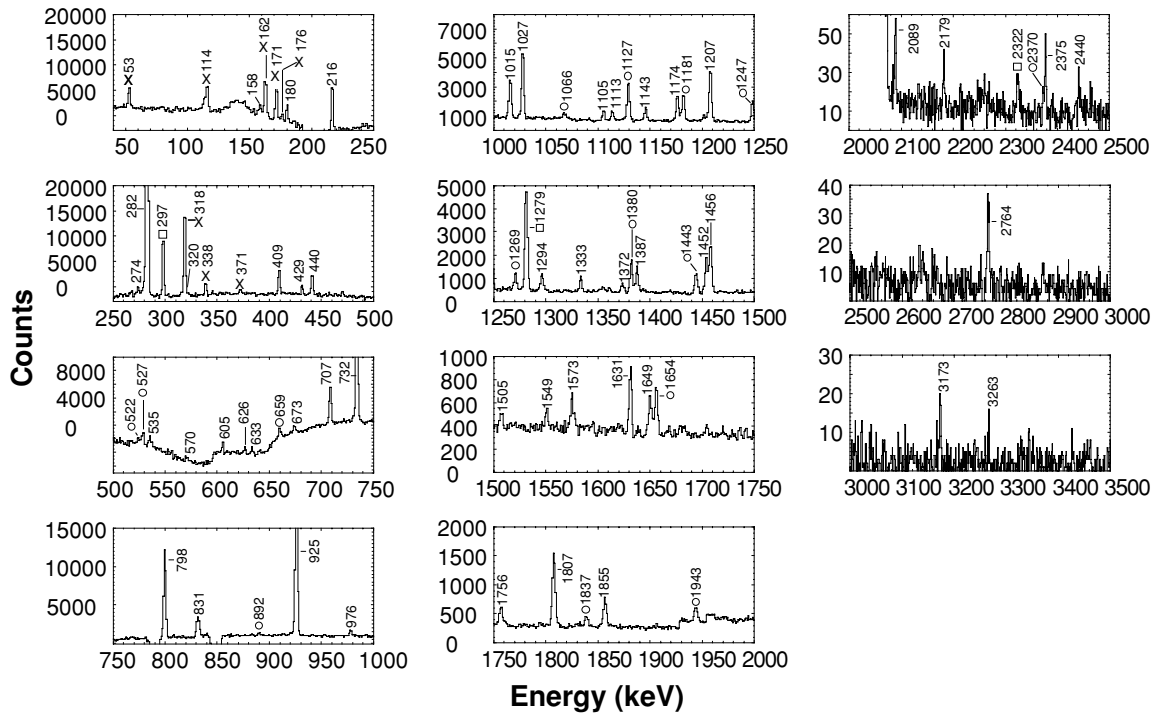


FIG. 1. A  $\gamma$  singles spectrum obtained by subtracting data taken with the laser off from data taken with the laser on at  $A = 135$ . Peaks associated with the  $\beta dn$  decay of  $^{135}\text{Sn}$  are labeled with “X”s, peaks corresponding to transitions in  $^{135}\text{Te}$  from the  $\beta$  decay of  $^{135}\text{Sb}$  are labeled with open circles, and peaks labeled with squares are transitions in  $^{134}\text{Te}$  from the  $\beta dn$  decay of  $^{135}\text{Sb}$ . The peaks shown at 2440, 2764, and 3263 keV were not placed in the decay scheme.

and  $\gamma$ - $\beta$  coincidence data were collected with both the laser-on and laser-off. The tape was moved after each measurement period to avoid buildup of long-lived isobaric activity in front of the detectors.

### III. RESULTS

The  $\gamma$ -ray spectrum obtained by subtracting a spectrum taken with the laser off from a spectrum taken with the laser on at  $A = 135$  is shown in Fig. 1. Only peaks associated with the decay of  $^{135}\text{Sn}$ , its daughters, and granddaughters should remain in the difference spectrum. The absence of the strong peaks at 787 and 846 keV from the decay of  $^{135}\text{Cs}^m$  illustrates the effectiveness of the use of the neutron converter to lower the presence of spallation produced nuclei. The peaks in Fig. 1 labeled by an “X” designate transitions that have been identified as  $\gamma$  rays which depopulate levels in  $^{134}\text{Sb}$  from the  $\beta dn$ -decay of  $^{135}\text{Sn}$  [11]. The peaks labeled with open circles correspond to transitions in the granddaughter nucleus,  $^{135}\text{Te}$  following  $\beta$  decay of  $^{135}\text{Sb}$ . The remaining unlabeled lines are tentatively assigned as  $\gamma$  rays which depopulate levels in  $^{135}\text{Sb}$ .

To distinguish the transitions in Fig. 1 that belong to the decay of  $^{135}\text{Sn}$  from those that can be attributed to the growth and decay of the  $^{135}\text{Sb}$  daughter; a difference spectrum (shown in Fig. 2) was obtained by subtracting the  $\gamma$  spectrum taken between 800 and 1000 ms following implantation from a  $\gamma$  spectrum taken between 50 and 250 ms following

implantation. This approach reduces or eliminates the  $\gamma$  rays arising from the growth and decay of 1.7-s  $^{135}\text{Sb}$  to levels of  $^{135}\text{Te}$  and other daughter nuclides.

The observed transitions assigned to the  $\beta$  decay of  $^{135}\text{Sn}$  into levels of  $^{135}\text{Sb}$  are shown in Fig. 3, and listed in Table I. The spectrum of  $\gamma$  rays in coincidence with the 282-keV transition in  $^{135}\text{Sb}$  is shown in Fig. 4. The 733-, 925-, 1105-, 1174-, 1452-, and 1807-keV  $\gamma$  rays were previously identified by Shergur *et al.* [9]. Peaks at 180, 1573, and 1756 keV correspond to transitions depopulating previously established levels at 1207, 1855, and 2089 keV, respectively. The 158-, 831-, and 976-keV lines were used to establish or support the placement of new levels at 440 and 1113 keV that also depopulate directly to the ground state.

The spectrum of  $\gamma$  rays in coincidence with the 440-keV transition in  $^{135}\text{Sb}$  is shown in Fig. 5(a). The peaks at 1294 and 1649 keV in Fig. 5(a) are transitions that depopulate known levels at 1734 and 2089 keV, respectively. The coincidence with the 673-keV  $\gamma$  ray and the presence of an 1113-keV  $\gamma$  ray in Figs. 1 and 2 supports the placement of a level at 1113 keV that, as noted above also depopulates to the level at 282 keV by the 831-keV  $\gamma$  ray. The 976-keV peak in Fig. 4 would then be likely to depopulate the 2089 keV level to the new 1113-keV level. The peak at 1391 keV provides support for the placement of a new level at 1831 keV. In addition, a peak at 913 keV supports placement of a level at 1353 keV.

Shown in Fig. 5(b) is a gate on the 707-keV  $\gamma$  ray. The 707-keV  $\gamma$  ray was previously identified by Bhattacharyya *et al.* as the  $11/2^+$  to  $7/2^+$  member of the yrast band [7].

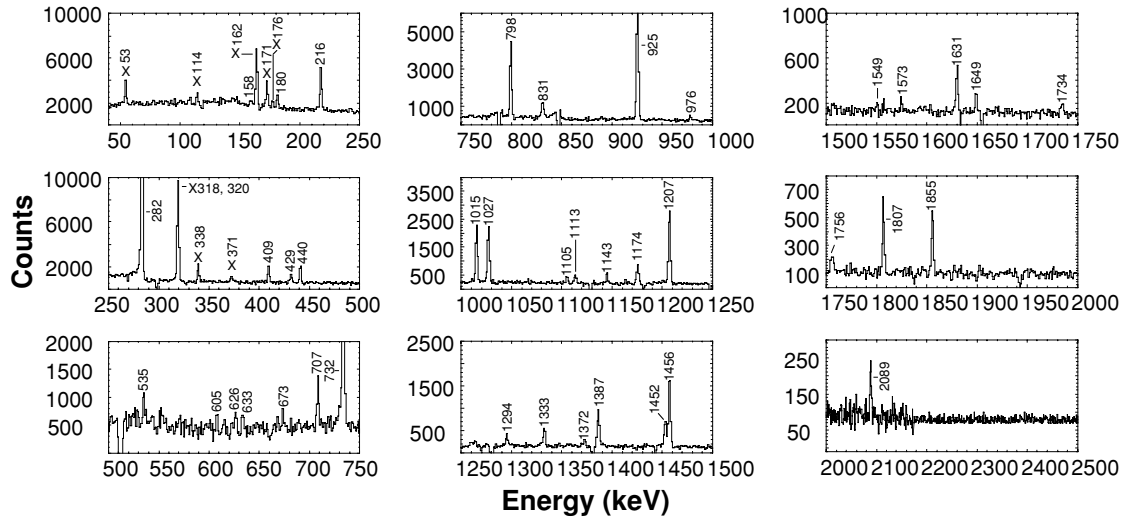
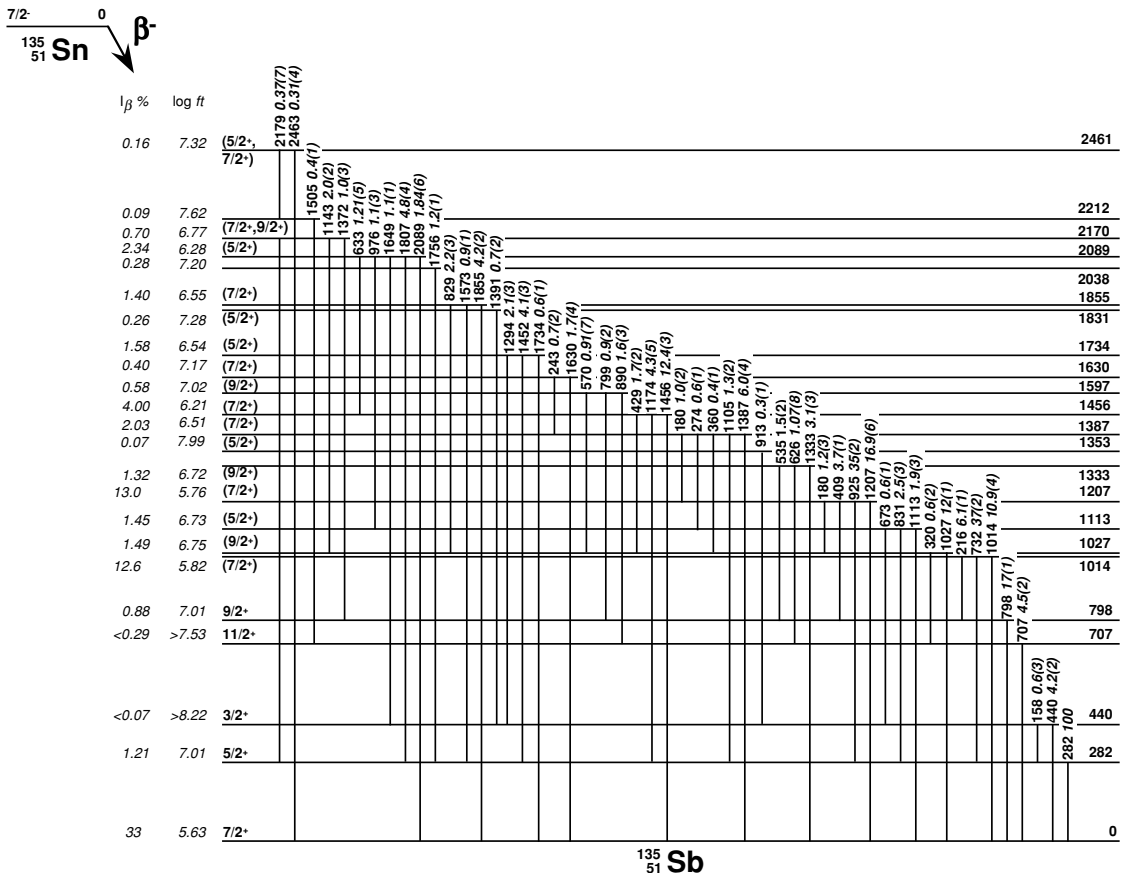


FIG. 2. A  $\gamma$  singles spectrum obtained by subtracting laser-on data obtained during the last 200 ms of a 1.0-s acquisition from data taken during the first 200 ms of the same acquisition. As in Fig. 3, peaks that can be attributed to transitions in the  $\beta$ dn-decay daughter,  $^{134}\text{Sb}$ , are labeled by an “X.”

The 626- and 890-keV peaks suggest new levels at 1333 and 1597 keV, respectively. The 411-keV  $\gamma$  ray identified by Bhattacharyya *et al.* as the  $15/2^+$  to  $11/2^+$  transition was not observed in this coincidence spectrum. A peak at 1505 keV

is also observed in the 707-keV gated spectrum that provides support for a level at 2212 keV.

The gate on the 798-keV transition is shown in Fig. 6 and includes two prominent  $\gamma$ -ray peaks at 216 and 409 keV that



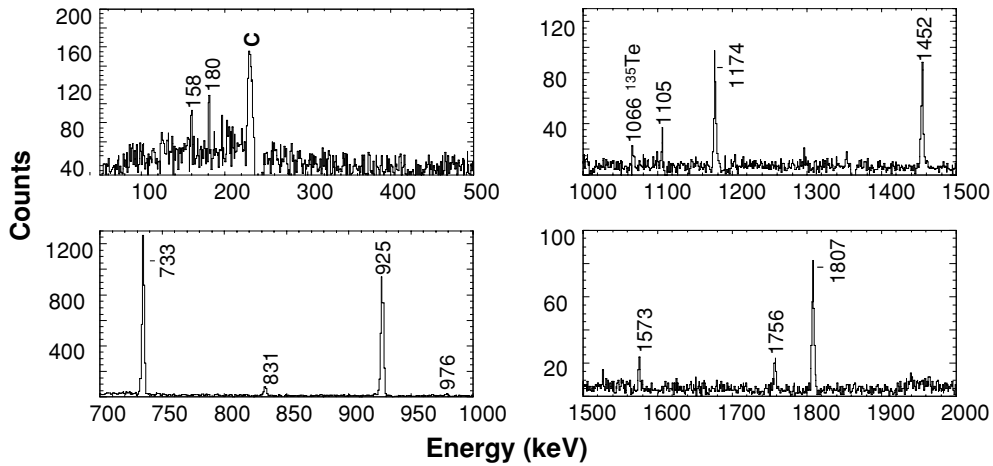


FIG. 4.  $\gamma$ - $\gamma$  coincidence spectrum gated on the 282-keV  $\gamma$ -ray transition in  $^{135}\text{Sb}$  following  $\beta$  decay of  $^{135}\text{Sn}$ .

populate the 798-keV level from previously identified levels at 1015 and 1207 keV. These coincident relationships taken in conjunction with the presence of an intense 798-keV peak in the  $\gamma$  singles spectrum provide evidence for a new level at 798 keV. The 535- and 799-keV peaks in Fig. 6 provide further evidence for the 1333- and 1597-keV levels, respectively; and the 1372 keV line establishes the position of a new level at 2170 keV. Peaks at 570 and 605 keV can be attributed to the  $\beta$  decay of  $^{134}\text{Cs}$  and are part of a 569-796-605 keV  $\gamma$  cascade.

In Fig. 7 gates are shown on the second and third most intense  $\gamma$  rays, the previously reported 732 and 925 keV transitions. The gate on the 732-keV  $\gamma$  ray in Fig. 7(a) shows no new coincidence relationships, and depopulates the level at 1015 keV. The gate on the 925-keV  $\gamma$  ray in Fig. 7(b) shows only one new coincidence relationship with a 180-keV  $\gamma$  ray, which would depopulate the established 1387 keV level.

Shown in Fig. 8(a), is a spectrum gated on the 831-keV  $\gamma$  ray, which is actually an unresolved 829-831 keV doublet. The peak at 976 keV would support the previously mentioned placement of a transition which depopulates the 2089-keV level. The presence of both the 282 and 1027 keV peaks further support the notion of a doublet  $\sim$ 830 keV. A  $\gamma$  spectrum gated on the 1027-keV transition is shown in Fig. 8(b). Peaks at 180, 360, 429, and 829 keV can be placed as depopulating previously established levels at 1207, 1387, 1456, and 1855 keV, respectively [9]. The 1143-keV line in the 1027-keV gated  $\gamma$  spectrum further supports the placement of a new level at 2170 keV, as suggested by the 798-1372 keV cascade. The 570-keV peak supports the previously placed level at 1597 keV.

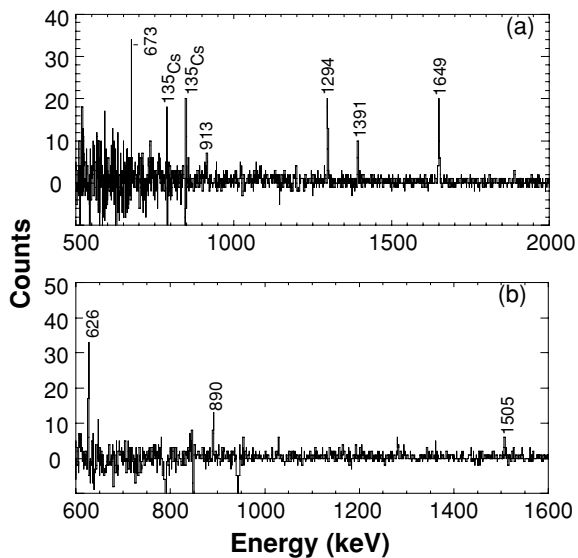


FIG. 5.  $\gamma$ - $\gamma$  coincidence spectra gated on the (a) 440- and (b) 707-keV  $\gamma$ -ray transitions in  $^{135}\text{Sb}$  following  $\beta$  decay of  $^{135}\text{Sn}$ .

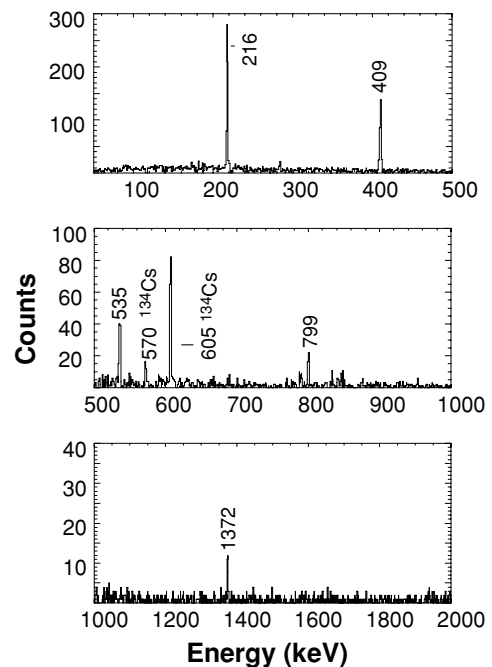


FIG. 6.  $\gamma$ - $\gamma$  coincidence spectrum gated on the 798-keV  $\gamma$ -ray transitions in  $^{135}\text{Sb}$  following  $\beta$  decay of  $^{135}\text{Sn}$ .

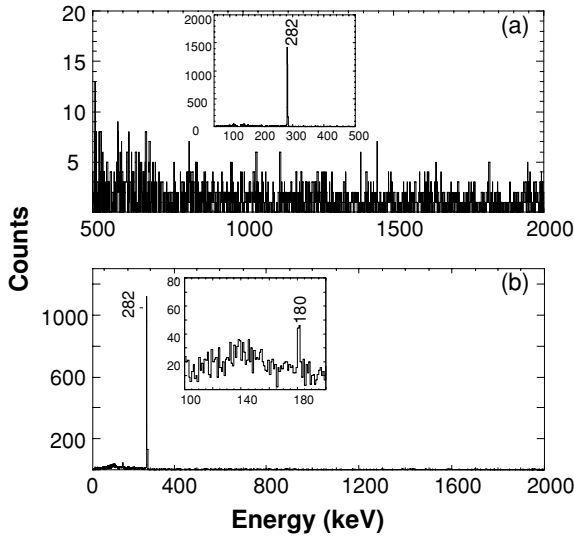


FIG. 7.  $\gamma$ - $\gamma$  coincidence spectra gated on the (a) 732- and (b) 925-keV  $\gamma$ -ray transitions in  $^{135}\text{Sb}$  following  $\beta$  decay of  $^{135}\text{Sn}$ .

IV. SPIN AND PARITY ASSIGNMENTS

In the previous experiment by Shergur *et al.* the first excited state at 282 keV was assigned a spin and parity of  $5/2^+$  [9]. This assignment was based on the apparent direct population in the  $\beta$  decay of  $7/2^-$   $^{135}\text{Sn}$ , and the absence of population of this level in the fission- $\gamma$  studies. Subsequently, Mach *et al.* reported a half-life of 6.0(7) ns for the 282-keV transition [12]. They noted that this  $T_{1/2}$  value indicates a rather low  $B(M1)$  value and also suggests that there is little collective  $E2$  enhancement for this transition. A low  $B(E2)$  value for this transition in  $^{135}\text{Sb}$  would also be consistent with the low  $B(E2)$  values found for the  $0^+$  to  $2^+$  transitions in isotonic  $^{134}\text{Sn}$  and  $^{136}\text{Te}$  [13]. In our recent study of the level structure of the adjacent odd-odd nuclide  $^{134}\text{Sb}$ , a number of  $E2$  transitions were identified ( $2^-$  to  $0^-$  and  $3^-$  to  $1^-$ ), and all were much

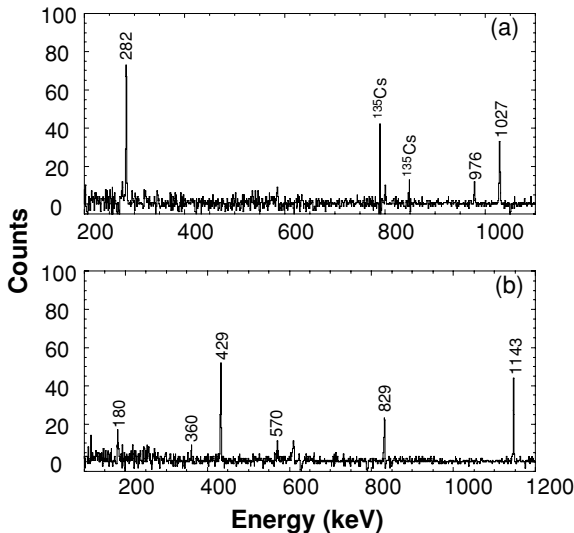


FIG. 8.  $\gamma$ - $\gamma$  coincidence spectra gated on the (a) 831- and (b) 1027-keV  $\gamma$ -ray transitions in  $^{135}\text{Sb}$  following  $\beta$  decay of  $^{135}\text{Sn}$ .

TABLE I. Data for  $\gamma$  rays and levels observed in the  $\beta$  decay of  $^{135}\text{Sn}$ .

Level (KeV)	$J^\pi$	$E_\gamma^a$	$I_\gamma^b$	Final state (keV)	$J^\pi$
282	$5/2^+$	282	100	0	$7/2^+$
440	$(3/2^+)$	440	4.1(2)	0	$7/2^+$
		158	0.6(3)	282	$5/2^+$
707	$11/2^+$	707	4.5(2)	0	$7/2^+$
798	$(9/2^+)$	798	17(1)	0	$7/2^+$
1014	$(7/2^+)$	1014	10.9(4)	0	$7/2^+$
		732	37(2)	282	$5/2^+$
		216	6.1(1)	798	$(9/2^+)$
1027	$(9/2^+)$	1027	12(1)	0	$7/2^+$
		320	0.6(2)	707	$11/2^+$
1113	$(5/2^+)$	1113	1.9(4)	0	$7/2^+$
		831	2.5(3)	282	$5/2^+$
		673	0.6(1)	440	$(3/2^+)$
1207	$(7/2^+)$	1207	16.9(6)	0	$7/2^+$
		925	35(2)	282	$5/2^+$
		409	3.7(1)	798	$(9/2^+)$
		180	1.2(3)	1027	$(9/2^+)$
1333	$(9/2^+)$	1333	3.1(3)	0	$7/2^+$
		626	1.07(8)	707	$11/2^+$
		535	1.5(2)	798	$(9/2^+)$
1353	$(5/2^+)$	913	0.3(1)	440	$(3/2^+)$
1387	$(7/2^+)$	1387	6.0(4)	0	$7/2^+$
		1105	1.3(2)	282	$5/2^+$
		360	0.4(1)	1027	$(9/2^+)$
		274	0.6(1)	1113	$(5/2^+)$
		180	1.0(2)	1207	$(7/2^+)$
1456	$(7/2^+)$	1456	12.4(3)	0	$7/2^+$
		1174	4.3(5)	282	$5/2^+$
		429	1.7(2)	1027	$(9/2^+)$
1597	$(9/2^+)$	890	1.6(3)	707	$11/2^+$
		799	0.9(2)	798	$(9/2^+)$
		570	0.91(7)	1027	$(9/2^+)$
1630	$(7/2^+)$	1630	1.7(4)	0	$7/2^+$
		243	0.7(2)	1387	$(7/2^+)$
1734	$(5/2^+)$	1734	0.6(1)	0	$7/2^+$
		1452	4.1(3)	282	$5/2^+$
		1294	2.1(3)	440	$(3/2^+)$
1831	$(5/2^+)$	1391	0.7(2)	440	$(3/2^+)$
1855	$(7/2^+)$	1855	4.2(2)	0	$7/2^+$
		1573	0.9(1)	282	$5/2^+$
		829	2.2(3)	1027	$(9/2^+)$
2038		1756	1.2(1)	282	$5/2^+$
2089	$(5/2^+)$	2089	1.84(6)	0	$7/2^+$
		1807	4.8(4)	282	$5/2^+$
		1649	1.1(1)	440	$(3/2^+)$
		976	1.1(3)	1113	$(5/2^+)$
		633	1.21(5)	1456	$(7/2^+)$
2170	$(9/2^+, 7/2^+)$	1372	1.0(3)	798	$(7/2^+)$
		1143	2.0(2)	1027	$(9/2^+)$
2212		1505	0.4(1)	707	$11/2^+$
2463	$(7/2^+, 5/2^+)$	2463	0.31(4)	0	$7/2^+$
		2179	0.37(7)	282	$5/2^+$
1549 <sup>c</sup>			0.43(5)		
2440 <sup>c</sup>			0.3(2)		

TABLE I. (*Continued.*)

Level (KeV)	$J^\pi$	$E_\gamma^a$	$I_\gamma^b$	Final state (keV)	$J^\pi$
2764 <sup>c</sup>			0.7(5)		
3263 <sup>c</sup>			0.5(2)		

<sup>a</sup>Uncertainty in  $\gamma$  ray energies is  $\pm 0.5$  keV.

<sup>b</sup>Relative to the 282-keV transition in  $^{135}\text{Sb}$ .

<sup>c</sup>High-energy transitions that are likely ground-state transitions that are not shown in the decay scheme as no other transitions were found that would depopulate such levels.

weaker than competing  $M1$  transitions ( $2^-$  to  $1^-$  and  $3^-$  to  $2^-$ ) [11].

In the analogous nuclide which has a single proton and two neutrons beyond double-magic  $^{208}\text{Pb}$ ,  $^{211}\text{Bi}$ , the  $B(M1)$  and  $B(E2)$  values measured for the decay of the first excited state at 405 keV are also small. The small  $B(M1)$  and  $B(E2)$  values measured for the decay of the 405-keV state in  $^{211}\text{Bi}$  are also slower than expected for a  $\Delta J = 1$  transition because the decay is hindered by the  $\Delta\ell = 2$  between the single-particle  $f_{7/2}$  and  $h_{9/2}$  states.

Below, we propose a set of spin and parity assignments for the levels that is based on the notion that  $E2$  transitions in the  $N = 84$  isotone  $^{135}\text{Sb}$  are not enhanced by significant collectivity and, in general, not competitive with possible  $M1$  transitions. Similarly lowered  $E2$  transition rates can also be seen in the decay of excited levels of isobaric  $^{135}\text{Te}$ . For example, the  $5/2^-$  level at 1654 keV depopulates by a 526-keV  $M1$  transition to the  $5/2^-$  level at 1127 keV with a relative intensity of 1.6 compared to  $E2$  transitions of 571 keV to the  $1/2^-$  level at 1083 keV, and 408 keV to the  $9/2^-$  level at 1246 keV, that have relative intensities of 0.043 and 0.071, respectively.

As the  $S_n$  for  $^{135}\text{Sb}$  is only 3.6 MeV, population of lower-energy levels by weak  $\gamma$ -ray transitions with intensities that are individually below the level of detection is much reduced for the decay of  $^{135}\text{Sn}$ . Indeed, population of levels above 3.6 MeV leads to the 21%  $P_n$  value that has been determined for  $^{135}\text{Sn}$  decay. Hence, we are treating the  $\beta$ -branching values shown in Fig. 3 to levels above 1 MeV that are over 0.1% and  $\log ft$  values under 8.00 as indication for first-forbidden, nonunique  $\beta$  decay that limits such levels to  $5/2^+$ ,  $7/2^+$ , and  $9/2^+$  spins and parities.

For example, the new level at 798 keV is seen to be populated directly in  $\beta$  decay, not populated in the yrast decay observed in the fission- $\gamma$  experiment, and does not depopulate to either the  $5/2^+$  level at 282 keV nor to the new level at 440 keV. Hence, it has been assigned a  $9/2^+$  spin and parity as the transition to the  $5/2^+$  level would be  $E2$ . In contrast, the new level at 440 keV is not populated in  $\beta$  decay which suggests a spin and parity of  $1/2^+$  or  $3/2^+$ , or  $11/2^+$  or above. As the 440-keV level is not populated in the yrast cascade and depopulates to both the  $7/2^+$  ground state and  $5/2^+$  level at 282 keV, it is tentatively assigned as a  $3/2^+$  level.

For the levels above 1.0 MeV, tentative spin and parity assignments have been made on the basis that the observed  $\gamma$  rays are  $M1$  transitions. Thus, the levels at 1014, 1207, 1387, 1456, and 1855 keV that depopulate to lower energy  $5/2^+$ ,  $7/2^+$ , and  $9/2^+$  levels are all given tentative ( $7/2^+$ ) spin and parity assignments. The level at 1027 keV that feeds the  $11/2^+$  level and not the  $5/2^+$  level is assigned a tentative  $J^\pi = 9/2^+$ , as is the 1333-keV level that depopulates to  $7/2^+$ ,  $9/2^+$ , and  $11/2^+$  levels. Levels at 2170 and 2461 keV that depopulate only to levels with two different spin and parity assignments could have the same spins and parities that the daughter levels are given.

Five levels at 1113, 1353, 1734, 1831, and 2089 keV depopulate to the  $3/2^+$  level at 440 keV, do not depopulate to the  $9/2^+$  level at 798 keV, and also appear to be directly populated in  $\beta$  decay, hence, all are given tentative  $5/2^+$  spin and parity assignments. The level at 1597 keV depopulates to the  $9/2^+$  and  $11/2^+$  levels at 798 and 707 keV, respectively, and also appears to be directly populated in  $\beta$  decay, hence it is assigned a tentative spin and parity of  $9/2^+$ .

With the spins and parities assigned as noted above, the  $\beta$  branching can be seen to strongly favor population of levels with  $7/2^+$  spin and parity, showing strong branches to the ground state and levels at 1014 and 1207 keV with  $\log ft$  values of 5.63, 5.82, and 5.76, respectively. Whereas, population of the three proposed  $5/2^+$  levels at 282, 1113, and 1353 keV are found to have  $\log ft$  values of 7.01, 6.73, and 7.99, respectively. These values can be compared to the decay of the single  $f_{7/2}$  neutron in  $^{133}\text{Sb}$  where the  $7/2^+$  ground state and  $5/2^+$  level at 963 keV are populated with  $\log ft$  values of 5.44 and 6.05, respectively [14]. As can be seen, the  $\beta$ -decay rate to the  $7/2^+$  levels in  $^{135}\text{Sb}$  is consistent with the ground state population of  $^{133}\text{Sb}$ , the decay to the  $5/2^+$  levels is much weaker, and at about the same level as the population of the three lowest-energy proposed  $9/2^+$  levels that are populated with  $\log ft$  values of 7.01, 6.75, and 6.72.

## V. SHELL-MODEL CALCULATIONS

To further investigate the structure of the low-energy states in  $^{135}\text{Sb}$ , calculations were carried out in the proton-neutron formalism with the shell model code OXBASH [15]. The model space consists of a  $^{132}\text{Sn}$  closed core with ( $Z = 50$ ) valence protons in the ( $0g_{7/2}$ ,  $1d_{5/2}$ ,  $1d_{3/2}$ ,  $2s_{1/2}$ ,  $0h_{11/2}$ ) orbitals and ( $N = 82$ ) valence neutrons in the ( $1f_{7/2}$ ,  $2p_{3/2}$ ,  $2p_{1/2}$ ,  $0h_{9/2}$ ,  $1f_{5/2}$ ,  $0i_{13/2}$ ) orbitals. The ground-state binding energies used in this calculation were taken from the recent mass table of Audi *et al.* [17]. The relative single-proton binding energies of  $-9.66$ ,  $-8.70$ ,  $-7.22$ ,  $-7.32$ , and  $-6.87$  MeV were used for the  $0g_{7/2}$ ,  $1d_{5/2}$ ,  $1d_{3/2}$ ,  $3s_{1/2}$ , and  $0h_{11/2}$  orbitals, in the initial unshifted calculation. The observed levels of  $^{133}\text{Sn}$  provided the single-particle neutron energies of  $-0.89$ ,  $-2.46$ ,  $-0.45$ ,  $-1.60$ ,  $-0.80$ , and  $0.25$  MeV for the  $0h_{9/2}$ ,  $1f_{7/2}$ ,  $1f_{5/2}$ ,  $2p_{3/2}$ ,  $2p_{1/2}$ , and  $1i_{13/2}$  orbitals, respectively.

The residual two-body interaction was obtained by starting with a  $G$  matrix derived from a more recent CD-Bonn [16] nucleon-nucleon interaction, with  $^{132}\text{Sn}$  as a closed core. A harmonic oscillator basis was employed for the single-particle wave functions with an oscillator energy ( $\hbar\omega = 7.87$  MeV).

The  $G$ -matrix elements form in turn the starting point for a perturbative derivation of a shell-model effective interaction. In this work we derive the effective interaction for the above shell-model space by the  $\hat{Q}$ -box method which includes all so-called nonfolded diagrams through third-order in the interaction  $G$  and sums up the folded diagrams to infinite order [18,19]. This type of Hamiltonian has been used to describe spectra of tin isotopes from mass number  $A = 102$  to  $A = 130$  [19] and the  $N = 82$  isotones up to  $A = 146$  [20] with good agreement with data.

The results of the Hartree-Fock calculations that indicated that the low- $\ell$  single-particle  $d_{5/2}$  and  $d_{3/2}$  levels would be lowered relative to the higher- $\ell$   $h_{11/2}$  and  $g_{7/2}$  levels, owing to the high  $N/Z$  ratio, the neutron skin were presented in our previous paper [9]. At that time, there were questions as to whether the low position of the  $5/2^+$  level at 282 keV was a consequence of the neutron skin or a consequence of collective effects. The long half-life measured by Mach *et al.* and the low  $B(E2)$  value which shows little evidence for collective enhancements in these  $N = 84$  isotones, leave only the lowered single-particle  $d_{5/2}$  and  $d_{3/2}$  energies as a mechanism for moving the  $d_{5/2}$  level from 963 keV in  $^{133}\text{Sb}$  to 282 keV in  $^{135}\text{Sb}$  [12]. The next question of interest is how this lowering will affect the fits to other levels in  $^{135}\text{Sb}$ .

Two calculations were performed using the CD-Bonn interaction. All of the calculated levels below 2 MeV are tabulated in Table II for spins up to  $11/2^+$ . The results with the standard, unshifted, single-particle energies are shown in column (a), and the levels calculated with the  $d_{5/2}$  and  $d_{3/2}$  single-proton energies lowered by 300 keV are shown in column (b). The observed levels from both decay and fission [7] are shown in Fig. 9, along with the levels listed in column (b) which show the better agreement between the observed and calculated levels. It can be seen that there is a level-for-level fit for all of these levels except for the nonobservation of a  $5/2^+$  level calculated at 1242 keV, and for the lowest  $1/2^+$  level calculated to be at 527 keV.

The effect of the lowering of the  $d_{5/2}$  and  $d_{3/2}$  single proton levels has been highlighted in Table II by showing the difference between the calculated values of (a) and (b) in column (d) of Table II. There was some judgment involved in associating the calculated levels with the observed levels. For example, the calculated  $5/2^+$  level in column (b) at 1478 keV was assumed to be not observed, and the  $5/2^+$  level at 1734 keV was assumed to be associated with the calculated level at 1687 keV, rather than being 250 keV above the calculated level at 1478 keV. In contrast, nearly all of the  $9/2^+$  and  $7/2^+$  levels calculated below 2 MeV could be associated with observed levels, although the proposed ( $7/2^+$ ) level at 1549 keV was not supported by any additional data other than its presence in the  $\gamma$  singles spectrum, and lack of coincidences.

It can be seen in Table II that the overall fit for the levels in  $^{135}\text{Sb}$  is greatly improved by the lowering of the  $d_{5/2}$  and  $d_{3/2}$  levels. Although the spins and parities of these states are tentative, the observed level density for the states fed directly by  $\beta$  decay is in agreement with expectations. An immediate consequence of the lowered  $d_{5/2}$  and  $d_{3/2}$  single particle energies is that the 527-keV position of the first  $5/2^+$

TABLE II. Comparison of experimentally observed levels with the results of four shell-model calculations for levels in  $^{135}\text{Sb}$  up to 2.0 MeV. All energies shown are in MeV.

$J^\pi$	Exp	CD		KH (c)	(d) $\Delta[(a)-(b)]$
		Bonn (a)	Bonn (b)		
1/2+		0.633	0.527	0.735	0.106
1/2+		1.448	1.377	1.087	0.071
3/2+	0.440	0.438	0.408	0.557	0.030
3/2+		1.360	1.335	1.093	0.025
3/2+		1.470	1.372	1.329	0.098
3/2+		1.867	1.837	1.690	0.030
3/2+			1.950	1.849	
5/2+	0.282	0.527	0.316	0.36	0.211
5/2+	1.113	1.212	1.188	0.831	0.024
5/2+	1.353 <sup>a</sup>	1.249	1.242	1.198	0.007
5/2+		1.468	1.478	1.281	–
					0.010
5/2+	1.734	1.885	1.687	1.419	0.198
5/2+	1.831 <sup>a</sup>	1.943	1.805	1.771	0.138
7/2+	0	0	0	0	
7/2+	1.014	1.135	1.134	0.982	0.001
7/2+	1.207	1.246	1.254	1.158	–
					0.008
7/2+	1.456	1.571	1.361	1.191	0.210
7/2+	(1.549)	1.592	1.537	1.342	0.055
7/2+	1.630	1.647	1.585	1.513	0.062
7/2+	1.855	1.963	1.835	1.673	0.128
9/2+	0.798	0.947	0.869	0.876	0.078
9/2+	1.027	1.165	1.039	1.055	0.126
9/2+	1.383	1.495	1.494	1.218	0.001
9/2+	1.597 <sup>a</sup>	1.784	1.783	1.647	0.001
9/2+		1.920	1.914	1.797	0.006
11/2+	0.707	0.662	0.666	0.729	–
					0.004
11/2+		1.643	1.621	1.459	0.022
11/2+		1.665	1.658	1.563	0.007
11/2+		1.813	1.779	1.661	0.034

<sup>a</sup>These levels have ambiguous  $J^\pi$  assignments, but are tentatively assigned based on  $\beta$  feeding, and the levels to which they deexcite. The level at 1549 keV is in parentheses, as the data for levels are not that extensive.

level shown in column (a) is pushed down to 316 keV in column (b) to be in better agreement with the observed  $5/2^+$  level at 282 keV. In column (d), it can be seen that the  $7/2^+$  level in column (b) at 1361 keV, the  $5/2^+$  level at 1687 keV, and the  $5/2^+$  level at 1805 keV are all lower by  $\sim 200$  keV relative to the levels in column (a), and all are in better agreement with the observed levels. Three other levels, the  $7/2^+$  level shown in column (b) at 1836 keV and the  $9/2^+$  levels at 855 and 1043 keV, are all seen to be lowered by  $\sim 100$  keV, and, again, all are in better agreement with observed levels.

For the levels that are not much changed by the lowering of the  $d_{5/2}$  and  $d_{3/2}$  single proton levels, reasonably good agreement is seen below 1500 keV for the  $3/2^+$  level, the other two excited  $7/2^+$  levels, and for the second excited  $5/2^+$  level.

		1254	7/2 <sup>+</sup>				
		<u>1242</u>	<u>5/2<sup>+</sup></u>	1247	6 <sup>+</sup>		
1207	7/2 <sup>+</sup>	1188	5/2 <sup>+</sup>				
		1134	7/2 <sup>+</sup>				
1117	15/2 <sup>+</sup>	<u>1088</u>	<u>15/2<sup>+</sup></u>	1073	4 <sup>+</sup>		
1113	5/2 <sup>+</sup>	1039	9/2 <sup>+</sup>				
1027	9/2 <sup>+</sup>						
<u>1014</u>	<u>7/2<sup>+</sup></u>						
		869	9/2 <sup>+</sup>				
798	9/2 <sup>+</sup>						
707	11/2 <sup>+</sup>			725	2 <sup>+</sup>		
		<u>666</u>	<u>11/2<sup>+</sup></u>				
		527	1/2 <sup>+</sup>				
440	3/2 <sup>+</sup>	<u>408</u>	<u>3/2<sup>+</sup></u>				
		316	5/2 <sup>+</sup>				
282	5/2 <sup>+</sup>						
0	7/2 <sup>+</sup>	0	7/2 <sup>+</sup>	0	0 <sup>+</sup>		
	<sup>135</sup> Sb		<sup>135</sup> Sb		<sup>134</sup> Sn		
	exp		CD Bonn		exp		

FIG. 9. Comparison of the experimental levels up to 1250 keV for <sup>135</sup>Sb with shell-model calculations using the CD Bonn interaction with a  $d_{5/2}$  single-particle energy lowered by 300 keV. Shown to the far right is the known level structure of <sup>134</sup>Sn.

In view of the success of the Kuo-Herling interaction used to describe the levels in <sup>134</sup>Sb by Shergur *et al.* [11], the fit for the structure of <sup>135</sup>Sb using the same TBME was investigated. In this calculation, the CD-Bonn proton-neutron interaction was replaced using the Kuo-Herling TBME, while still using the CD-Bonn neutron-neutron TBME. The levels calculated for <sup>135</sup>Sb in this manner are tabulated in column (c) in Table II by using  $1d_{3/2}$  and  $1d_{5/2}$  proton single-particle energies lowered by 300 keV. As can be seen in column (c), the use of the KH  $pn$  interactions has the general effect of lowering the positions of many of the excited levels by 100 to 200 keV. In particular, the second  $5/2^+$  level is calculated to be at 831 keV, well below the 1113-keV position of the level that is assigned as the second  $5/2^+$  level. Whereas, the second  $7/2^+$  and the first and second  $9/2^+$  levels are at about the same energies in both calculations and also are in reasonably good agreement with the observed levels. In contrast, the lowest  $3/2^+$  calculated energy is pushed up by almost 200 keV to a position at 557 keV, well above the observed position at 440 keV.

As this approach has not resulted in a better overall fit for the levels of <sup>135</sup>Sb, we conclude that the scaling used for this interaction that was assumed by Chou and Warburton [4] is apparently not needed. It would appear that the higher overlap of the proton-neutron wave functions in <sup>132</sup>Sn compared to

<sup>208</sup>Pb that follows from the oscillator model is cancelled by the effects of the neutron skin in <sup>132</sup>Sn. The more recent renormalized  $G$  matrix obtained by Hjorth-Jensen from the CD-Bonn potential that was used in the calculations in columns (a) and (b) of Table II has bare  $G$  matrix elements that are similar to Kuo-Herling but has higher-order renormalizations that in total are different from the first-order corrections used for the Kuo-Herling calculations. Although it should be expected that going to higher order is better, there appear to be dependencies on the underlying single-particle spectrum that need further investigation [16]. The CD-Bonn renormalized  $G$  matrix gives better agreement for the  $T = 1$  spectrum of <sup>132</sup>Sn than obtained with Kuo-Herling [11]. Therefore, a consistent Hamiltonian for this mass region has yet to be found.

## VI. SUMMARY AND OUTLOOK

New data have been taken at CERN/ISOLDE for the decay of mass separated <sup>135</sup>Sn using a neutron converter to dramatically lower isobaric Cs contamination. From these time dependent  $\gamma$ -ray singles and  $\gamma$ - $\gamma$  coincidence spectra, positions for five of the six levels calculated by the CD Bonn potential for <sup>135</sup>Sb below 1.0 MeV have been established and many of the  $5/2^+$ ,  $7/2^+$ , and  $9/2^+$  levels that could be directly populated in  $\beta$  decay between 1 and 2 MeV have also been identified. Tentative spin and parity assignments have been proposed for most levels assuming that  $M1$  transitions dominate the deexcitation of the levels in <sup>135</sup>Sb. Of importance was the identification of the  $3/2^+$  and  $9/2^+$  levels at 440 and 798 keV, respectively, which allowed for more stringent testing of the single particle energies and TBME used in this mass region.

Comparison of the predictions between the CD Bonn and Kuo-Herling interactions showed that the observed levels of <sup>135</sup>Sb were best reproduced by using the CD Bonn proton-neutron TBME instead of the Kuo-Herling proton-neutron TBME. Moreover, the effect of the 300-keV lowering of the  $d_{5/2}$  and  $d_{3/2}$  single-proton orbitals in order to provide better agreement for the observed 282-keV position of the lowest  $5/2^+$  level is seen to lead to the lowering of six other levels, all of which are in better agreement with observed levels. In contrast, recent calculations for the level structure of <sup>135</sup>Sb reported by Sarker and Sarker that were performed with the unshifted  $d_{5/2}$  single-proton energy result in an energy of either 618 or 690 keV for the position of the lowest  $5/2^+$  level [22].

There are also good prospects for observation of the predicted low-energy  $1/2^+$  and  $3/2^+$  levels via  $\beta$ -delayed neutron decay from <sup>136</sup>Sn and comparisons with the calculated level positions shown in Table II. Just as the  $\beta$ -delayed neutron decay of <sup>135</sup>Sn populated additional levels in <sup>134</sup>Sb that were not observed in the direct  $\beta$  decay of <sup>134</sup>Sn [11], decay of  $0^+$  <sup>136</sup>Sn can be expected to populate  $1^+$  levels via Gamow-Teller transitions that lie above the neutron separation energy in <sup>136</sup>Sb. These  $1^+$  levels can, in turn, be expected to emit  $\ell = 0$  neutrons and populate low-energy  $1/2^+$  and  $3/2^+$  levels in <sup>135</sup>Sb. Such levels should be easily identified by gating on the low-energy  $5/2^+$  and  $3/2^+$  levels at 282 and 440 keV identified in this study.



## ACKNOWLEDGMENTS

This work was supported by the U.S. Department of Energy, office of Nuclear Physics under Contract Nos. W-31-109-EN6-39 and DE-FG02-94-ER40834; the German Bundesministerium für Bildung und Forschung (BMBF) under Contract No. 06MZ-864; the National Science

Foundation under Contracts Nos. PHY0070911 and PHY0140324; and by the EU-RTD project TARGISOL (HPRI-2001-50033). The authors acknowledge the support of the ISOLDE staff during the experiment, and W.B.W. also wishes to acknowledge the support of the Alexander von Humboldt Foundation for support for work in Germany and Europe.

- 
- [1] B. Pfeiffer *et al.*, Nucl. Phys. **A693**, 282 (2001).  
[2] I. Dillmann *et al.*, Phys. Rev. Lett. **91**, 162503 (2003).  
[3] E. K. Warburton and B. A. Brown, Phys. Rev. C **43**, 602 (1991).  
[4] W.-T. Chou and E. K. Warburton, Phys. Rev. C **45**, 1720 (1992).  
[5] S. Sarkar and M. S. Sarkar, Phys. Rev. C **64**, 014312 (2001).  
[6] J. H. Hamilton *et al.*, Eur. Phys. J. A **15**, 175 (2002).  
[7] P. Bhattacharyya *et al.*, Eur. Phys. J. A **3**, 109 (1998).  
[8] J. Shergur *et al.*, Nucl. Phys. **A682**, 493 (2001).  
[9] J. Shergur *et al.*, Phys. Rev. C **65**, 034313 (2002).  
[10] A. Korgul, H. Mach, B. Fogelberg, W. Urban, W. Kurcewicz, and V. I. Isakov, Phys. Rev. C **64**, 021302(R) (2001).  
[11] J. Shergur *et al.*, Phys. Rev. C, in press (2005).  
[12] A. Korgul *et al.*, Eur. Phys. J. A direct, in press (2005).  
[13] D. C. Radford *et al.*, Phys. Rev. Lett. **88**, 222501 (2002).  
[14] M. Sanchez-Vega, B. Fogelberg, H. Mach, R. B. E. Taylor, A. Lindroth, J. Blomqvist, J. Covello, and A. Gargano, Phys. Rev. C **60**, 024303 (1999).  
[15] A. Etchegoyen *et al.*, MSU-NSCL Report No. 524, 1985.  
[16] M. Hjorth-Jensen, private communication (2004).  
[17] G. Audi, A. H. Wapstra, and C. Thibault, Nucl. Phys. **A729**, 337 (2003).  
[18] M. Hjorth-Jensen *et al.*, Phys. Rep. **261**, 125 (1995).  
[19] M. Hjorth-Jensen *et al.*, J. Phys. G **22**, 321 (1996).  
[20] A. Holt *et al.*, Nucl. Phys. **A634**, 41 (1998).  
[21] A. Holt *et al.*, Nucl. Phys. **A618**, 107 (1998).  
[22] S. Sarkar and M. S. Sarkar, Eur. Phys. J. A **21**, 61 (2004).